

We are IntechOpen, the world's leading publisher of Open Access books Built by scientists, for scientists

5,900

Open access books available

145,000

International authors and editors

180M

Downloads

Our authors are among the

154

Countries delivered to

TOP 1%

most cited scientists

12.2%

Contributors from top 500 universities



WEB OF SCIENCE™

Selection of our books indexed in the Book Citation Index
in Web of Science™ Core Collection (BKCI)

Interested in publishing with us?
Contact book.department@intechopen.com

Numbers displayed above are based on latest data collected.
For more information visit www.intechopen.com



Anterior Chamber Angle Assessment Techniques

Claudio Campa, Luisa Pierro, Paolo Bettin and Francesco Bandello
 Department of Ophthalmology, University Vita-Salute, Scientific Institute San Raffaele
 Milan,
 Italy

1. Introduction

The anterior chamber angle is the actual anatomical angle created by the root of the iris and the peripheral corneal vault. Within it lie the structures involved in the outflow passage of the aqueous, namely the trabecular meshwork and the Schlemm's canal (figure 1).

The depth of the angle in a healthy eye is approximately 30°, with the superior part usually less deep than the inferior half. However the depth is influenced by gender, age and refractive error. Female gender has the greatest influence on iridocorneal angle reduction, followed by age and spherical equivalent (Rufer et al.).

The relationship of the iris plane to the cornea has a significant effect on the aqueous humor's accessibility to its outflow drainage system. In eyes where the iris and corneal endothelium are "closed" against one another, the aqueous will not be drained causing an increase of the intraocular pressure (angle closure glaucoma) (Lens, 2008).

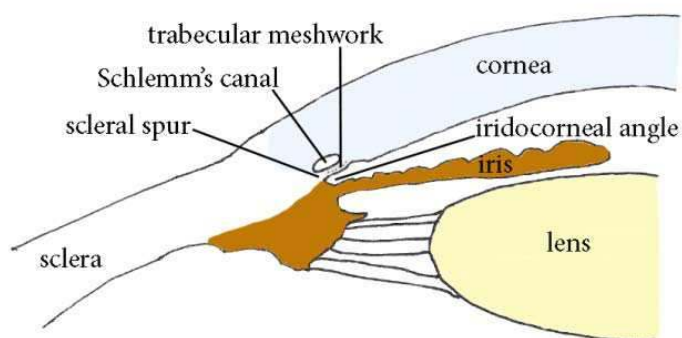


Fig. 1. Diagram of the anatomical structures forming the iridocorneal angle

Primary angle-closure glaucoma (PACG) is a leading cause of blindness worldwide (Quigley and Broman, 2006). Five overlapping conditions, not necessarily progressing in an orderly sequence, are usually described in this disease: angle closure suspect, intermittent (subacute) angle closure, acute angle closure, chronic angle closure and absolute angle closure (Kanski, 2007).

At the earliest stage (angle closure suspect), eyes have narrow or occludable angles without raised intraocular pressure (IOP) or glaucomatous optic neuropathy. It has been estimated that

22% of the eyes with angle closure suspect progress to acute angle closure (Thomas et al., 2003a) whereas 28.5% progress to chronic angle closure over 5–10 years (Thomas et al., 2003b). Prophylactic laser iridotomy performed in eyes with narrow angles may halt the progression of the angle closure process and prevent development of PACG (Nolan et al., 2003). Similarly peripheral iridoplasty, which may also be used to break an attack of acute angle-closure unresponsive to medical therapy or laser iridotomy, can be successfully employed in nonacute situations in patients with angle-closure when laser iridotomy fails to deepen the anterior chamber angle, i.e. particularly in case of plateau iris (Ritch et al., 2007, Ng et al., 2008).

Hence evaluation of anterior chamber angle (ACA) is of great importance to identify and treat those patients at risk for PACG.

It is well known that the depth and volume of the anterior chamber diminish with age and are related to the degree of ametropia. Male subjects have larger anterior chamber dimensions than female subjects. Although grading of limbal chamber depth using van Herick's technique (see below) is commonly used as a surrogate for measuring ACA, gonioscopy has represented for many years the only method able to adequately quantify ACA. However this technique has a subjective and semi-quantitative nature, is hardly reportable due to the difficulty of obtaining good images and requires a good training to be performed properly.

Moreover, in some circumstances such as plateau iris, the angle can be narrow despite a deep anterior chamber. For these reasons, with technology advancements, several new techniques have been proposed with the aim of providing a better imaging of the anterior segment. In this chapter we will show the clinical findings of each method reviewing the strengths and limitations of each approach.

2. van Herick test

Performed on the slit lamp without any additional aids, the van Herick test allows quick, not invasive assessment of anterior angle width. The technique was originally described by van Herick (Van Herick et al., 1969): a narrow slit of light is projected onto the peripheral nasal or temporal cornea at an angle of 60° as near as possible to the limbus. This results in a slit image on the surface of the cornea the width of which is compared with the peripheral anterior chamber depth ("black space") (figure 2). A four-point scale is then used, with each grade indicating the probability of angle closure. In grade 4 the anterior chamber depth (ACD) is $\geq 100\%$ corneal thickness and the angle is wide open; in grade 3 it is > 25 to 50% and the angle is incapable of closure; in grade 2 it is 25% and the angle closure is possible; in grade 1 is $< 25\%$ and the angle closure is likely.

Studies have shown suboptimal results when using van Herick test to screen for primary angle closure (Alsbirk, 1986), (Congdon et al., 1997), (Thomas et al., 1996): particularly it has been found that measurements performed at the nasal limbus tend to overestimate the angle width. To improve precision in quantification of ACD, Foster (Foster et al., 2000a) proposed a modified scheme in which the original grade 1 was sub-divided into 0%, 5%, and 15% corneal thickness, and a grade of 75% corneal thickness was added to compensate for the gap between the original grades 3 and 4. This seven-point grading system resulted in 99% sensitivity compared to gonioscopic evaluation; the interobserver agreement for this augmented grading scheme was good (weighted kappa 0.76). However it is hardly reproducible in clinical practice.



Fig. 2. An example of van Herick technique for assessing anterior chamber depth (a grade 4 is shown, see text)

3. Smith method

Another optical technique used to determine ACD is Smith's slit-length method (Smith, 1979). It is performed using a standard slit-lamp. The illumination system is located in the subject's temporal field at an angle of 60° and the slit-beam is projected horizontally. If measuring the patient's right eye the right ocular of the slit lamp is used and vice versa for the left eye. A beam of approximately 1.5 mm thickness, with its orientation horizontal, is placed across the cornea. The procedure involves focusing the slit-beam on the corneal surface while an out of focus image of the slit-beam is observed on the iris/lens surface. The length of the slit-beam when the two corneal and iris/lens images are just touching is multiplied by a constant to give the ACD in millimetres (figure 3). In the original description of the method by Smith the constant was 1.40, while others (Barrett et al., 1996) have proposed more recently 1.31. Both constants have been determined using an optical pachymetry.

The Smith method has been validated by a number of authors (Barrett et al., 1996) (Douthwaite and Spence, 1986). It allows the clinician to obtain reliable estimates of axial ACD, without any attachments to the slit-lamp biomicroscope. The axial ACD estimates are accurate to within ± 0.25 mm (Smith, 1979), ± 0.2 mm (Jacobs, 1979) and ± 0.33 mm (Barrett et al., 1996) as compared to pachymetry and to within ± 0.42 mm, as compared to ultrasonography. There is no effect of the central corneal thickness on the ACD estimate made using this method (Osuobeni et al., 2003), which has also a minimum inter and intra observer variation (Osuobeni et al., 2000).

From birth to the age of 13 years, the mean value of ACD increases from 2.37 to 3.70 mm for Northern European boys, and from 2.39 to 3.62 mm for girls (Larsen, 1971). There is very little change in the mean anterior chamber depth from the teenage years to about 30 years, while there is a decline in the mean anterior chamber depth from 30 to 60 years, probably because of the increase of lens thickness (Fontana and Brubaker, 1980). Between this age range the typical value is around 2.5 mm. The depth and volume of the anterior chamber are also related to the degree of ametropia. Male subjects usually have larger anterior chamber dimensions than female subjects. There is a direct association between narrow anterior chamber angle and shallow anterior chamber depth (Wishart and Batterbury, 1992).

Consequently, the ACD quantification represents an indirect means of assessing the anterior chamber angle and identifying patients who are more likely to develop PACG. Usually eyes with ACD <2 mm are considered at risk (Wishart and Batterbury, 1992).



Fig. 3. Measurement of the anterior chamber depth using Smith's method. Yellow arrow indicates the focused horizontal corneal-imaged slit and red arrow the out-of-focus iris/lens-imaged slit (see text for details)

4. Gonioscopy

Gonioscopy still represents the gold standard for assessment of the angle. This technique was first developed by Trantas in the late 1800s and subsequently modified by Koeppe and Barkan to allow a direct visualization of the structure of the anterior chamber angle with a contact lens (Friedman and He, 2008). Nowadays however indirect gonioscopy (which relies on mirrors or prisms to reflect light from the angle to the viewer) is usually preferred because of several advantages over direct gonioscopy: the patient can be examined at the slit lamp using a variable magnification and there is no astigmatic aberration. Two lenses are commonly employed: the Zeiss-type and the Goldmann-type. The Zeiss-type lens has a 9-mm diameter corneal surface (radius of curvature 7.72 mm) and doesn't require a coupling agent. The Goldmann-type has larger base diameter (corneal surface 12 mm and radius of curvature 7.38 mm) and requires a coupling agent (thick artificial tears or hydroxypropyl methylcellulose) when placed on the cornea. Although use of Zeiss-type lens needs more training and expertise, it has undoubted advantages because leaves the anterior segment clear for later viewing of the posterior pole and compresses the cornea centrally, which in turns allows for greater dynamic assessment of the angle structures.

Moreover pressure on the larger base lenses can lead to compression over Schwalbe's line with a consequent alteration of angle's morphology.

Since illumination conditions and degree of pupil dilation may dramatically alter angle configuration, a strict assessment protocol should be followed: the patient should look straight ahead and should be examined in a dark room, using a 1-mm beam with adequate illumination to visualize angle structures (Weinreb and Friedman, as cited in (Friedman and He, 2008)).

Three grading systems have been proposed for documenting angle findings seen in gonioscopy: Scheie (Scheie, 1957), Schaffer (Shaffer, 1960) and Spaeth (Spaeth, 1971) classification (table 1).

Scheie		Schaffer			Spaeth		
Classification	Findings	Classification	Findings	Angle width (deg.)	Classification	Findings	
Wide open	All structures visible	Grade 4	Ciliary body is visible	35-45	Iris insertion	A	Anterior
						B	Behind
						C	In sclera
						D	Deep angle recess
						E	Extremely deep recess
Grade I	Iris root not visible	Grade 3	Scleral spur is visible	20-35	Width of angle recess	0, 10, 20, 30 and 40 degrees	
Grade II	Ciliary body not visible	Grade 2	Only trabecular meshwork is visible	20	Peripheral iris configuration	S	Steep
						R	Regular
						Q	Queer
Grade III	Posterior trabecular meshwork not visible	Grade 1	Only Schwalbe's line is visible	≤ 10	12 o'clock pigmentation	0	None
						1+	Just visible
						2+	Mild
						3+	Moderately dense
						4+	Dense
Grade IV	None of angle structures visible	Grade 0	Angle is closed	0			

Table 1. Angle grading systems

In the Scheie scheme grade zero represents a wide open angle. Grade 1 is a "slightly narrow" angle and the iris root is not visible; grade 2 means that the ciliary body is not visible while grade 3 means that the posterior (pigmented) trabecular meshwork is not visible. Grade 4 is a closed angle and therefore no angle structures are visible. Scheie believed that persons with grade 3 and grade 4 angles were at greatest risk of PACG.

The Shaffer system is currently the most popular grading system. It uses both angle width and angle structures to classify angle grade: this is confusing because sometimes width and structures seen may place an angle into different categories. In this grading system angles between 35 and 45 degrees are classified as grade 4, those between 20 and 35 as grade 3, those between 10 and 20 as grade 2 and those ≤10 as grade 1, with a closed angle (zero degrees) classified as grade 0. Angle width is often preferred to angle depth in the description of ACA, because the latter may differ in different locations. Taking into consideration the angle structures, Shaffer classification's grade 4 comprises all structures, grade 3 the structures up to the scleral spur, grade 2 up to the trabecular meshwork, in grade 1 only the Schwalbe's line is visible and in grade 0 none of the angle structures are visible.

Spaeth classification provides the most comprehensive approach to angle assessment. This classification includes three components: angular width of angle recess, configuration of the peripheral iris, insertion site of the iris root. The width of the angle recess is graded from 10 to 40 degrees. The iris configuration is reported as "r" (regular), "s" (steep, as in plateau iris configuration), or "q" (queer, or backward, bowing as may occur in pigment dispersion syndrome). The insertion of iris root ranges from A - anterior to the Schwalbe's line, B - behind Schwalbe's line, but anterior to scleral spur, C - posterior to scleral spur (i.e., scleral spur visible, but not ciliary body), D - ciliary body visible, and E - large amount of ciliary body visible. When the iris is appositional with the angle, the "apparent" iris insertion, seen

without indentation, is noted as a letter placed in parenthesis, while the “actual” insertion is noted with a letter not placed in parenthesis. Finally the Spaeth system rates also the pigment of the posterior trabecular meshwork at 12 o’clock from 0 to 4+ (black pigmented meshwork) and the presence or absence of peripheral anterior synechiae (PAS). An example of wide open angle is given in figure 4.



Fig. 4. Gonioscopy of a wide open angle. All angle structures are visible. From down to top: ciliary body band with some iris processes reaching the trabecular meshwork, scleral spur, pigmented (posterior) trabecular meshwork, nonpigmented (anterior) trabecular meshwork and Schwalbe's line delineated by some scattered pigment

Not many studies have been published on the reliability of the angle grading systems. Some authors have reported a weighted k values for inter-observer reproducibility of Shaffer classification in the ranges of 0.6 using a Goldmann-style lens (Foster et al., 2000b) (Aung et al., 2005). The Spaeth system has shown high reproducibility and comparability to UBM in 22 patients (Spaeth et al., 1995).

A quantitative grading of the angle has been proposed by some authors (Cockburn, 1980, Congdon et al., 1999), but has not gained popularity in clinical practice.

Once an angle is viewed and it is determined that there is iridotrabecular contact, it is necessary to determine whether the angle is appositionally closed or if there are permanent PAS. To pursue this task a gentle indentation with the goniolens is performed (“dynamic gonioscopy”). By indenting the central cornea (usually with a Zeiss-type lens) the aqueous is displaced into the peripheral anterior chamber where it bows the iris posteriorly and widens the chamber angle. This widening differentiates areas where the peripheral iris is permanently adherent to the peripheral cornea (i.e. PAS) from areas where the iris is merely reversibly apposed to the peripheral cornea.

Caution must be taken in distinguishing PAS from iris processes. Iris processes, either plastered across the surface of the angle or bridging from the peripheral iris to the angle structures, are pigmented strands continuous with and histologically identical to the iris. These are a normal variant and have no effect upon aqueous outflow. On the contrary PAS are abnormal adhesions of the peripheral iris to the angle structure that, if extensive enough, can eventually reduce trabecular outflow. Usually PAS tend to be wider (at least half of 1 clock hour in width) and are present to the level of the trabecular meshwork or higher.

Examples of PAS include the fibrovascular membrane formed in neovascular glaucoma, proliferating abnormal endothelial cells in the iridocorneal endothelial (ICE) syndromes, epithelialization of the angle due to epithelial ingrowth, or inflammatory trabecular and keratic precipitates in contact with an inflamed iris in uveitis.

The gonioscopic criteria for an occludable angle usually include: 1) trabecular meshwork invisible in 270° or more of the entire angle in the primary position of gaze without indentation and / or 2) angular width less than 20 degrees by the Shaffer grading (Kim and Jung, 1997). Often these criteria are used to identify angles that require treatment (i.e. iridotomy), although there is still no unanimous consensus (Friedman, 2001, Foster et al., 2002).

5. Pentacam

The Pentacam (Oculus, Inc., Lynnwood, WA, USA) is a rotating Scheimpflug camera with a short-wavelength slit light (475 nm, blue light-emitting diode laser) that is able to take 25 slit images of the anterior segment of the eye in 2 seconds with 500 true elevation points in each image. Any eye movement is detected (and the results corrected) by a second camera. A three-dimensional model of the anterior segment can therefore be built with the obtained data including the corneal thickness, corneal topographic parameters, central ACD, anterior chamber angle (ACA), anterior chamber volume (ACV) and other parameters. Interestingly the software doesn't require any manual initiation. Two chamber angles for each chosen meridian are provided. It is noteworthy to mention that ACA is calculated by lengthening the posterior cornea and the iris contour to compute the chamber angle using an interpolation method, because Pentacam cannot image the angle recess and scleral spur. Several studies have investigated the reliability of Pentacam (and other Scheimpflug cameras) in measuring ACA. Lam (Lam et al., 2002) found on 25 healthy subjects with open angles that the 95% limit of agreement on repeat measurements of angle width was 5°, and inter-observer agreement was 6°. Rabsilber showed good reliability of Pentacam in assessing ACA in 76 healthy volunteers (Rabsilber et al., 2006). Although measurement of the ACA obtained with the Pentacam seem to correlate significantly with Shaffer's grade determined by gonioscopy, a certain discrepancy has been reported between ACA and ACD measured by Pentacam and ultrasound biomicroscopy (UBM) or anterior-segment optical coherence tomography (AS-OCT) in eyes with a narrow angle (Liang et al.) (Kurita et al., 2009) (Mou et al.). This may be due to the inability of the Pentacam to visualize the most peripheral part of the iris. Alternatively the placement of an eye cup, which is necessary for UBM examination, may be responsible of a flattening of the cornea which in turns leads to an artificial reduction of the ACD. Hence ACV seems to be the most efficient parameter to screen patients with POAG or POAG suspect using the Pentacam (Kurita et al., 2009). However although Pentacam non-contact approach to angle assessment is highly appealing for screening purposes, it is limited to visualization of only the angle recess. Scheimpflug photography indeed does not display the retroiridal structures or the ciliary body, which are of great interest in glaucoma diagnosis.

6. Ultrasound Biomicroscopy (UBM)

Ultrasound-based diagnostic imaging uses a probe containing a piezoelectric transducer to emit a sound wave which propagates through tissues and is partially reflected –echoes-

from anatomic structures differing in acoustic impedance (density \times speed of sound). Some of the echoes return to the transducer and are converted back into voltages and amplified. The range of each echo is proportional to the time delay between sound wave emission and echo return, specifically, $r = ct/2$, where r is the range, c is the speed of sound (1532 m/s at 37°C in normal saline) and t is the time (Ursea and Silverman).

Each pulse/echo event thus provides information along one line of sight. By mechanically scanning the probe, information along an ordered series of lines is obtained. By converting echo amplitude into pixel intensity, a 2D cross-sectional B-scan image is then produced.

Ultrasonic imaging resolution improves by increasing the frequency of the transducer. However higher frequencies produce a correspondingly smaller wavelength which is less able to penetrate the tissues.

Ultrasound systems utilizing probes of approximately 35 MHz or more have come to be known as “ultrasound biomicroscopy” (UBM) or ‘very high-frequency ultrasound systems’. Such systems have a tissue penetration of only 5 mm but provide lateral and axial resolutions approximately of 40 and 20 microns, respectively. They allow therefore for a more detailed assessment of the anterior ocular structures than was available using traditional B-scan ultrasound.

UBM systems are now produced by numerous companies, with probes ranging from 50 to 80 MHz. Handheld UBM probes are now often equipped with acoustically transparent, fluid-filled ‘bubble tips’ that can be placed directly onto the globe. These obviate the use of water-baths or scleral shells for acoustic coupling, greatly simplifying the examination and allowing the patient to be examined in a sitting position.

UBM provides both quantitative and qualitative information on the anterior segment of the eye. Pavlin and coworkers carried out the first clinical UBM study of the ocular structures in glaucomatous patients in the early 1990s (Pavlin et al., 1992). Subsequently many authors proposed different biometric parameters to characterize the angle and anterior segment. The most common include: angle-opening distance (AOD), trabecular-iris angle (TIA), trabecular-ciliary process distance (TCPD), iris thickness (ID), angle-recess area (ARA), iris ciliary process distance (ICPD), iris-lens contact distance (ILCD) (see Table 2 and figure 5 for details).

AOD and ARA can be measured at various distances from the sclera spur. Theoretically, 500 μm is the appropriate distance because it approximates the length of the trabecular meshwork. However, a longer measurement distance of 750 μm uses information from a large region of the image and may be more robust, especially for ARA, since it is less affected by local iris surface undulations. Henzan and coworkers studied the performance of the UBM parameters in differentiating primary angle closure/primary angle closure suspect from non-occludable angle eyes through the receiver operating characteristic (ROC) curve and the area under the curve (AUC). They found that AOD₅₀₀ and TIA under light conditions had the greatest AUC of 0.94. The ideal cutoff values for the AOD₅₀₀ and TIA under light conditions determined with the Youden index (=sensitivity - [1 - specificity]) were 0.17 mm (sensitivity, 0.82; specificity, 0.96) and 15.2 degrees (sensitivity, 0.83; specificity, 0.93), respectively (Henzan et al.).

A limitation of these findings is that UBM measurements of angle structures can be influenced by a number of variables including patient’s age and gender (Friedman et al., 2008), direction of gaze, accommodation, room illumination, variation in image acquisition (position of the probe, meridians scanned) (Friedman and He, 2008).

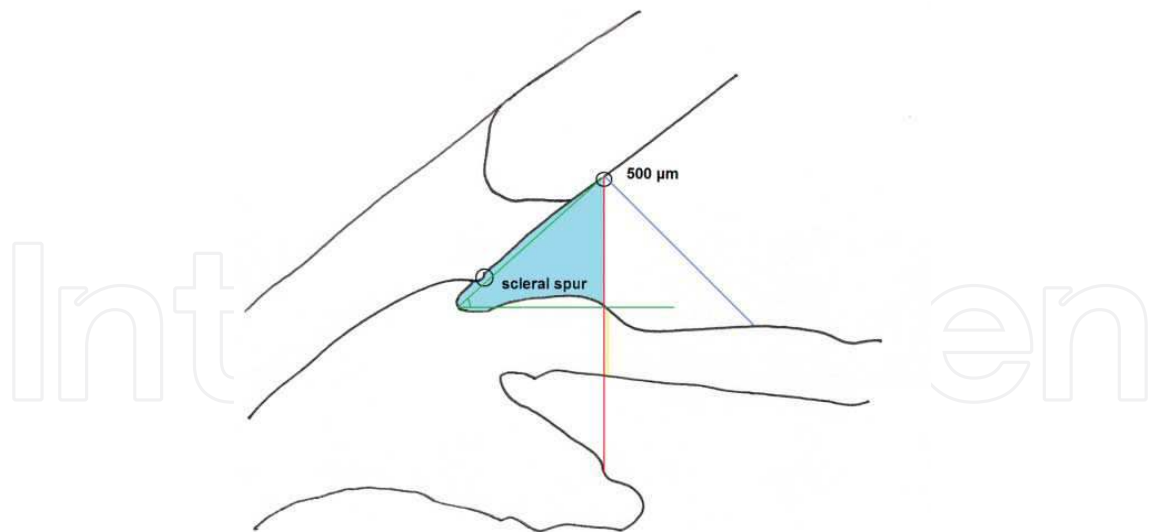


Fig. 5. Diagram illustrating several biometric descriptors of the angle, including angle-opening distance (blue line), iris thickness (yellow line), trabecular-iris angle (red line), trabecular-ciliary process distance (green line) and angle recess area (light blue area). In this example measurements are made 500 μm from the sclera spur

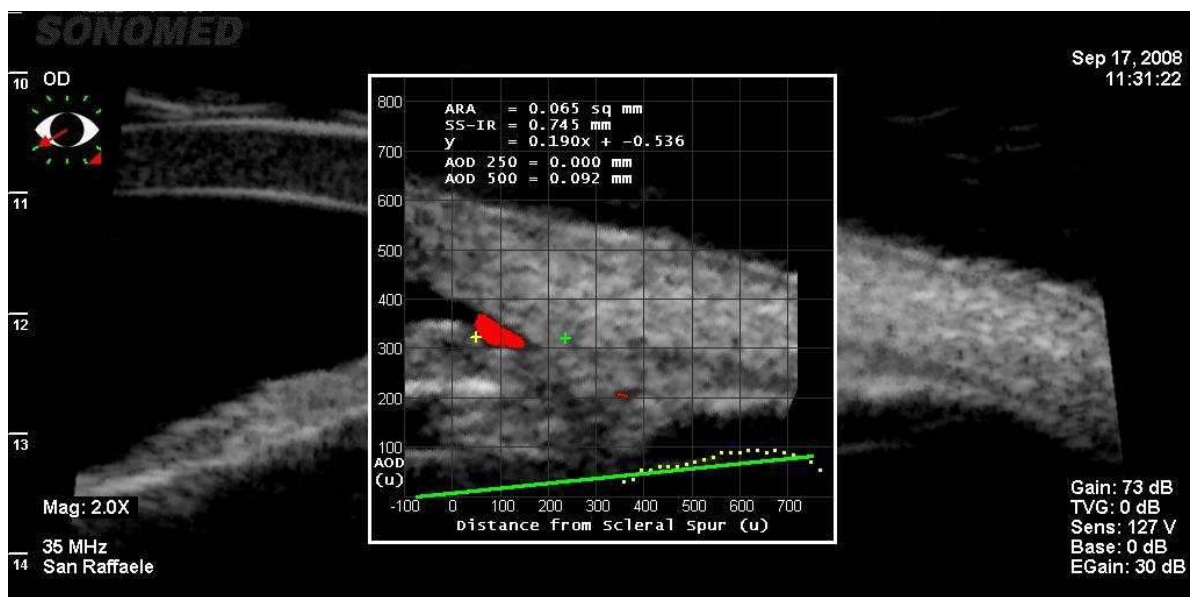


Fig. 6. Screen shot of the analysis software from the UBM Pro 2000 (UBM Pro 2000, Paradigm Medical Industries, Salt Lake City, UT, USA)

One would expect high variability in the measurements because of the partly subjective nature of the caliper placement on visualized anatomic landmarks. On the contrary the reported reproducibility of analyses on single UBM images seems to be pretty good. Marchini showed high reproducibility in a paper comparing UBM parameters in angle closure patients (range of coefficient of variation 1.4 -16%) (Marchini et al., 1998). Even better reproducibility was reported by Gohdo when measuring the ciliary body thickness (CBT) one and two millimeters posterior to the scleral spur (coefficient of variation < 2.5%) (Gohdo et al., 2000).

In any case image analysis using calipers to mark each structure takes a large amount of time due to the need to place a cursor at each point for any given measurement.

To overcome this issue, Ishikawa and colleagues created a semi-automated program (UBM Pro 2000, Paradigm Medical Industries, Salt Lake City, UT, USA) that provides several important parameters once the scleral spur is identified (figure 6) (Ishikawa et al., 2000).

Parameter	Description	Range*		References
		Occludable angle (OA)	Nonoccludable angle (NOA)	
AOD ₅₀₀	Distance from cornea to iris at 500 μm from the scleral spur	0.11 \pm 0.04	0.29 \pm 0.13	(Henzan et al.)
TIA	Angle formed from angle recess to points 500 μm from scleral spur on corneal endothelium and perpendicular on surface of iris	10.3 \pm 3.9	24.2 \pm 9.3	(Henzan et al.)
TCPD	Measured from point on endothelium 500 μm from scleral spur perpendicularly through iris to ciliary process	0.62 \pm 0.11	0.77 \pm 0.16	(Henzan et al.)
ID	Measured from perpendicular 500 μm from scleral spur	0.40 \pm 0.05	0.41 \pm 0.05	(Henzan et al.)
ARA ₇₅₀	Area of triangle between angle recess, iris and cornea 750 μm from scleral spur	0.10 \pm 0.08	0.13 \pm 0.01	(Friedman et al., 2003) for NOA (Yoo et al., 2007) for OA
ICPD	Distance from the posterior iris surface to the ciliary process perpendicular 500 μm from scleral spur	0.39 \pm 0.21	0.40 \pm 0.10	(Sihota et al., 2005)
ILCD	Length of contact between surfaces of lens and iris	0.79 \pm 0.22	0.98 \pm 0.41	(Sihota et al., 2005)

*All values (mean \pm standard deviation) are in mm except TIA which is in degrees and ARA₅₀₀ which is in mm².

Abbreviations: AOD=angle-opening distance; TIA=trabecular-iris angle; TCPD=trabecular-ciliary process distance; ID:iris thickness; ARA=angle-recess area; ICPD=iris ciliary process distance; ILCD=iris-lens contact distance;

Table 2. Biometric parameters used in UBM for characterizing the angle and anterior segment in subjects with an occludable/nonoccludable angle

The software calculates AOD₂₅₀, AOD₅₀₀, ARA₇₅₀ and performs linear regression analysis of consecutive AODs, producing two figures: the acceleration and the y-intercept. Acceleration tells how rapidly the angle is getting deeper, using the tangent of the angle instead of degrees as the unit. The y-intercept refers to the distance between the scleral spur and the iris surface along the perpendicular to the trabecular meshwork plane.

Acceleration and the y-intercept can be negative numbers. A negative number for acceleration means that the angle has an almost normal configuration at its peripheral part and becomes very shallow or is attached to the cornea at its central part. A negative y-intercept means that the angle recess is very shallow or is attached to the cornea at its periphery, whereas it is relatively wide centrally. According to Ishikawa and colleagues this software dramatically improves the overall reproducibility, with a coefficient of variation ranging between 7.3 and 2.5 for the various parameters (Ishikawa et al., 2000).

UBM gives also valuable qualitative information which helps in the diagnosis and in the management of several ocular diseases. In plateau iris syndrome UBM well demonstrates the ciliary body anteriorly positioned compressing the iridocorneal angle and placing the peripheral iris in apposition to the trabecular meshwork (figure 7).

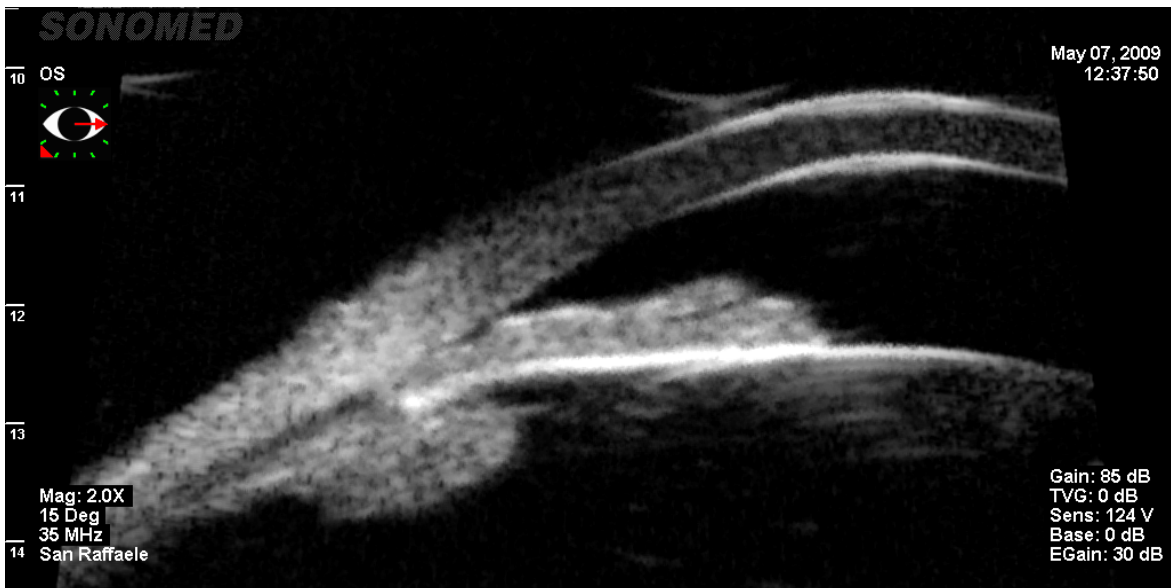


Fig. 7. Ultrasound biomicroscopy view of an eye with plateau iris syndrome

In pigment dispersion syndrome UBM shows an open angle, a characteristic concave iris and a ciliary body rotated posteriorly (figure 8).

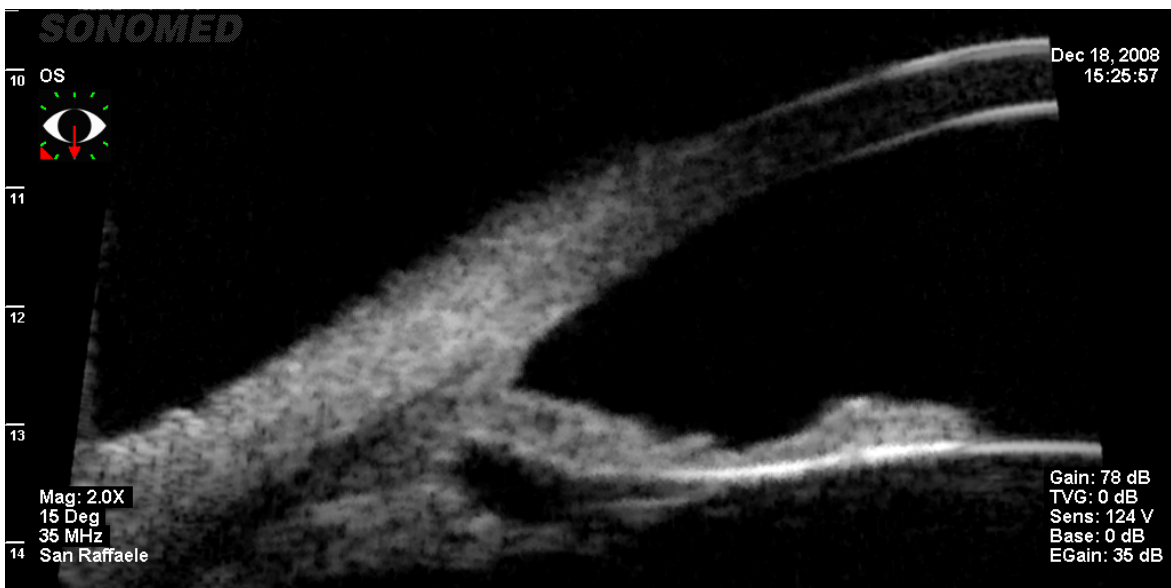


Fig. 8. Ultrasound biomicroscopy view of an eye with pigment dispersion syndrome

Angle recession, intraocular foreign bodies, ciliary body cysts are also easily detectable by UBM. Lastly UBM may represent a useful tool for the planning and guidance of glaucoma surgery, including the evaluation of filtering blebs, sclerectomy and canaloplasty, as well as the diagnosis and evaluation of postoperative complications.

7. Anterior segment optical coherence tomography (AS-OCT)

Optical coherence tomography (OCT) of the eye was first described by Huang and coworkers at the Massachusetts Institute of Technology (Boston, MA, USA) in 1991 (Huang et al., 1991). OCT uses a near-infrared light that is directed throughout ocular tissues. While most of the light is absorbed by the tissues or scattered, a small portion is reflected and collected by an interferometer in order to produce an image. In time-domain OCT, the reference mirror is mechanically scanned in the range axis, and this allows determination of the range to optical reflections along the tissue path, which are represented by interference fringes in the OCT signal.

OCT was initially developed only for retinal imaging; in 1994 Izatt et al. (Izatt et al., 1994) for the first time used it also for imaging the anterior chamber (anterior segment OCT, AS-OCT). Since then, AS-OCT has rapidly become popular for ACA assessment.

Originally anterior and posterior segment imaging used the same wavelength (830 nm). Subsequently a longer wavelength of 1310 nm was preferred for AS-OCT. This increases the depth of penetration by reducing the amount of light scattered by the sclera and limbus, allowing for visualization of the ACA morphology in greater detail. In addition, the 1310 nm light incident on the cornea is strongly absorbed by water in the ocular media, with only 10% reaching the retina. This enables the AS-OCT to utilize higher power, enhancing imaging speed and eliminating motion artifacts (Quek et al.). The Visante™ OCT (Carl Zeiss Meditec, Dublin, CA, USA) and the SL-OCT (Heidelberg Engineering, GmbH, Dossenheim, Germany) are 2 commercially available devices which use this wavelength providing an axial and transverse resolution of 18 μm and 60 μm , respectively, for the Visante and <25 μm and 20–100 μm for the SL-OCT (Quek et al.). SL-OCT incorporates OCT technology into a modified slit-lamp biomicroscopy system: this requires slower image acquisition speed and more operator skills.

More recently the new frequency (Fourier) domain OCTs have been developed, where the broadband signal is broken into a spectrum using a grating or linear detector array (i.e. sensitive detectors arranged in grating or single row), and depth is determined from the Fourier transform of the spectrum without motion along the reference arm (Ursea and Silverman). The fast readout speed of the detectors (typically tens of kilohertz) allows acquisition at video frame rates (30 fps) while the multiplexed scheme provides a signal-to-noise ratio (SNR) advantage over time domain OCT (TD-OCT). Fourier (also called Spectral) domain OCTs (SD-OCTs) allows scans at a rate of 26,000 A-scans per second and more images to be taken in a single pass. These devices produce therefore detailed cross-sectional images of structures at an axial resolution of 5 μm and a transverse resolution of 15 μm .

The RTVue (Optovue Inc., Fremont, CA, USA), the Cirrus high-definition OCT (HD-OCT) 4.0 (Cirrus; Carl Zeiss Meditec Inc.) and the OPKO Spectral OCT SLO (OPKO Health, Inc.) are all SD-OCT systems that can be used for either retinal or anterior segment imaging (when used with a corneal adaptor module).

AS-OCTs provide same type of ACA measurements of UBM, with the same advantages and limitations (i.e. they are influenced by patient's age and gender, direction of gaze, accommodation, room illumination, meridians scanned). Furthermore, likewise UBM, some AS-OCTs have a built-in semi-automated software which offers the most common biometric parameters of ACA after the manual localization of the scleral spur (figure 9) (table 3). Contradictory results are present in literature on the agreement between UBM and AS-OCT in quantitative ACA measurement and detection of narrow angles. Some authors have

found the two methods to be quite similar (Radhakrishnan et al., 2005, Dada et al., 2007); others have shown poor agreement (Mansouri et al.). In a study including 32 patients Wang et al. have reported that low-resolution OCT is similar to UBM for most of the studied angle measurements, while high-resolution OCT tends to give higher measurements than both low-resolution OCT and UBM. Furthermore AS-OCT measurements seem more reproducible than those from UBM (Wang et al., 2009). Likewise UBM, AS-OCT may be used for qualitative evaluation of ACA in a variety of ocular diseases (plateau iris syndrome, pigment dispersion syndrome, etc.) and it is undoubtedly safer than UBM in the evaluation of filtering blebs because AS-OCT is non-contact technique.

Parameter	Description	Range*		References
		Occludable angle (OA)	Nonoccludable angle (NOA)	
AOD _{500 nasal}	Distance from cornea to iris at 500 µm from the scleral spur	0.33±0.14	0.50±0.21	(Grewal et al.)
AOD _{500 temporal}	See above	0.30±0.11	0.51±0.22	(Grewal et al.)
TISA _{500nasal}	Trapezoidal area with the following boundaries: anteriorly, AOD ₅₀₀ ; posteriorly, a line drawn from the scleral spur perpendicular to the plane of the inner scleral wall to the opposing iris; superiorly, the inner corneo-scleral wall; and inferiorly, the iris surface.	0.23±0.14	0.34±0.11	(Grewal et al.)
TISA _{500temporal}	See above	0.23 ±0.14	0.33±0.12	(Grewal et al.)
ARA _{750 nasal}	Area of triangle between angle recess, iris and cornea 750 µm from scleral spur	0.08	0.29	(Pekmezci et al., 2009)
ARA _{750temporal}	See above	0.09	0.28	(Pekmezci et al., 2009)

*All values (mean±standard deviation) are in mm except ARA and TISA which are in mm².

Abbreviations: AOD=angle-opening distance; TISA=trabecular-iris space area; ARA=angle recess area;

Table 3. Most common biometric parameters used in AS-OCT for characterizing the angle and anterior segment in subjects with an occludable/non-occludable angle

Compared to UBM, AS-OCT is a technique more rapid, more easily practiced by a technician, better tolerated because requires no contact. A limitation of AS-OCT is that it doesn't allow visualizing the ciliary body and the supra-choroidal space. Using gonioscopy as reference standard several authors have shown sensitivities of AS-OCT in detecting narrow angles up to 98%, although often the specificity was significantly lower (between 55 and 85%) (Nolan et al., 2007, See et al., 2007) (Pekmezci et al., 2009). AS-OCT tends indeed to detect more closed ACAs than gonioscopy, particularly in the superior and inferior quadrants (Nolan et al., 2007, Sakata et al., 2008a).

Angle recess area at 750 µm from scleral spur (ARA₇₅₀) and angle-opening distance at 500 µm from the scleral spur (AOD₅₀₀) seem to have the highest correlation with gonioscopy (Pekmezci et al., 2009).

Radhakrishnan indicated an AOD 500 cutoff of 190 µm for detecting occludable angles (Radhakrishnan et al., 2005).

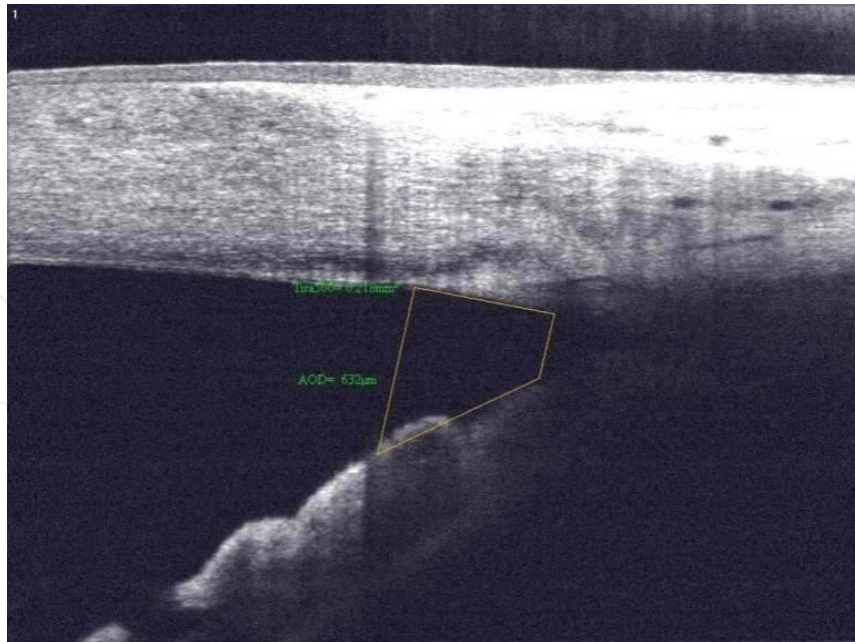


Fig. 9. Screen shot of the ACA measurements (angle-opening distance and trabecular-iris space area at 500) provided by the analysis software of RTVue OCT (Optovue Inc., Fremont, CA, USA)

As for UBM, also for AS-OCT angle classification hinges on accurate localization of the scleral spur, as it is used as the reference point for all the other quantitative measurements. However, this localization is not always easy to be found possibly generating non-negligible intra- and inter-observer variance.

The sclera spur can be defined as the point where there is a change in curvature of the inner surface of the angle wall, often appearing as an inward protrusion of the sclera.

Studies investigating the visibility of the sclera spur with AS-OCT showed a visualization between 70% and 78.9% of analyzed images (Sakata et al., 2008b) (Wong et al., 2009). Most of the cases in which the scleral spur could not be detected occurred in images in which the internal surface of the sclera formed a smooth continuous line (with no inward protrusion of the sclera or change in its curvature) or in images with suboptimal quality. Less frequently, the scleral spur was difficult to identify owing to an atypical contour of the inner corneoscleral wall.

Despite the possible difficulty in localization of sclera spur, several studies have shown low intra- and inter-observer variability of AS-OCT ACA measurements, which tends to increase only when AS-OCT image acquisitions are performed by less-experienced operators (Khor et al., Tan et al., Muller et al., 2006, Li et al., 2007) In a recent study the range of intra-observer variability in image analysis was from 9.4% to 12.5% in the experts and from 4.2% to 17.4% in the non-experts. Inter-observer variability was 10.7% in the experts and 10.2% in the non-experts. The reproducibility was high, 0.875 and 0.942 in the experts and 0.906 in the non-experts (Tan et al.).

8. Conclusions

Several new technologies are becoming more and more popular for the assessment of the angle and anterior segment. They can provide useful additional qualitative information to

those obtained with the traditional tools (slit-lamp and gonioscopy). Furthermore they can offer also precise ACA measurements which however are often not comparable each other. Hence we believe that one should build its normative data - using gonioscopy as reference standard- to use them for screening for angle closure purposes.

However, as technologies evolve, it is likely that the diagnostic performance of different techniques/instruments may soon reach acceptable specificity and sensitivity levels for mass screening for angle closure.

9. References

- Alsbirk, P.H. (1986). Limbal and axial chamber depth variations. A population study in Eskimos. *Acta Ophthalmol (Copenh)*, Vol. 64, No. 6, (Dec 1986) pp. (593-600), 0001-639X (Print)
- Aung, T., Lim, M.C., Chan, Y.H., Rojanapongpun, P. & Chew, P.T. (2005). Configuration of the drainage angle, intraocular pressure, and optic disc cupping in subjects with chronic angle-closure glaucoma. *Ophthalmology*, Vol. 112, No. 1, (Jan 2005) pp. (28-32), 1549-4713 (Electronic)
- Barrett, B.T., McGraw, P.V., Murray, L.A. & Murgatroyd, P. (1996). Anterior chamber depth measurement in clinical practice. *Optom Vis Sci*, Vol. 73, No. 7, (Jul 1996) pp. (482-486), 1040-5488 (Print)
- Cockburn, D.M. (1980). A new method for gonioscopic grading of the anterior chamber angle. *Am J Optom Physiol Opt*, Vol. 57, No. 4, (Apr 1980) pp. (258-261), 0093-7002 (Print)
- Congdon, N.G., Spaeth, G.L., Augsburger, J., Klancnik, J., Jr., Patel, K. & Hunter, D.G. (1999). proposed simple method for measurement in the anterior chamber angle: biometric gonioscopy. *Ophthalmology*, Vol. 106, No. 11, (Nov 1999) pp. (2161-2167), 0161-6420 (Print)
- Congdon, N.G., Youlin, Q., Quigley, H., Hung, P.T., Wang, T.H., Ho, T.C. & Tielsch, J.M. (1997). Biometry and primary angle-closure glaucoma among Chinese, white, and black populations. *Ophthalmology*, Vol. 104, No. 9, (Sep 1997) pp. (1489-1495), 0161-6420 (Print)
- Dada, T., Sihota, R., Gadia, R., Aggarwal, A., Mandal, S. & Gupta, V. (2007). Comparison of anterior segment optical coherence tomography and ultrasound biomicroscopy for assessment of the anterior segment. *J Cataract Refract Surg*, Vol. 33, No. 5, (May 2007) pp. (837-840), 0886-3350 (Print)
- Douthwaite, W.A. & Spence, D. (1986). Slit-lamp measurement of the anterior chamber depth. *Br J Ophthalmol*, Vol. 70, No. 3, (Mar 1986) pp. (205-208), 0007-1161 (Print)
- Fontana, S.T. & Brubaker, R.F. (1980). Volume and depth of the anterior chamber in the normal aging human eye. *Arch Ophthalmol*, Vol. 98, No. 10, (Oct 1980) pp. (1803-1808), 0003-9950 (Print)
- Foster, P.J., Buhrmann, R., Quigley, H.A. & Johnson, G.J. (2002). The definition and classification of glaucoma in prevalence surveys. *Br J Ophthalmol*, Vol. 86, No. 2, (Feb 2002) pp. (238-242), 0007-1161 (Print)
- Foster, P.J., Devereux, J.G., Alsbirk, P.H., Lee, P.S., Uranchimeg, D., Machin, D., Johnson, G.J. & Baasanhu, J. (2000a). Detection of gonioscopically occludable angles and primary angle closure glaucoma by estimation of limbal chamber depth in Asians: modified grading scheme. *Br J Ophthalmol*, Vol. 84, No. 2, (Feb 2000a) pp. (186-192), 0007-1161 (Print)

- Foster, P.J., Oen, F.T., Machin, D., Ng, T.P., Devereux, J.G., Johnson, G.J., Khaw, P.T. & Seah, S.K. (2000b). The prevalence of glaucoma in Chinese residents of Singapore: a cross-sectional population survey of the Tanjong Pagar district. *Arch Ophthalmol*, Vol. 118, No. 8, (Aug 2000b) pp. (1105-1111), 0003-9950 (Print)
- Friedman, D.S. (2001). Who needs an iridotomy? *Br J Ophthalmol*, Vol. 85, No. 9, (Sep 2001) pp. (1019-1021), 0007-1161 (Print)
- Friedman, D.S., Gazzard, G., Foster, P., Devereux, J., Broman, A., Quigley, H., Tielsch, J. & Seah, S. (2003). Ultrasonographic biomicroscopy, Scheimpflug photography, and novel provocative tests in contralateral eyes of Chinese patients initially seen with acute angle closure. *Arch Ophthalmol*, Vol. 121, No. 5, (May 2003) pp. (633-642), 0003-9950 (Print)
- Friedman, D.S., Gazzard, G., Min, C.B., Broman, A.T., Quigley, H., Tielsch, J., Seah, S. & Foster, P.J. (2008). Age and sex variation in angle findings among normal Chinese subjects: a comparison of UBM, Scheimpflug, and gonioscopic assessment of the anterior chamber angle. *J Glaucoma*, Vol. 17, No. 1, (Jan-Feb 2008) pp. (5-10), 1057-0829 (Print)
- Friedman, D.S. & He, M. (2008). Anterior chamber angle assessment techniques. *Surv Ophthalmol*, Vol. 53, No. 3, (May-Jun 2008) pp. (250-273), 0039-6257 (Print)
- Gohdo, T., Tsumura, T., Iijima, H., Kashiwagi, K. & Tsukahara, S. (2000). Ultrasound biomicroscopic study of ciliary body thickness in eyes with narrow angles. *Am J Ophthalmol*, Vol. 129, No. 3, (Mar 2000) pp. (342-346), 0002-9394 (Print)
- Grewal, D.S., Brar, G.S., Jain, R. & Grewal, S.P. Comparison of scheimpflug imaging and spectral domain anterior segment optical coherence tomography for detection of narrow anterior chamber angles. *Eye (Lond)*, (Feb 18, 1476-5454 (Electronic)
- Henzan, I.M., Tomidokoro, A., Uejo, C., Sakai, H., Sawaguchi, S., Iwase, A. & Araie, M. Comparison of Ultrasound Biomicroscopic Configurations Among Primary Angle Closure, Its Suspects, and Nonoccludable Angles: The Kumejima Study. *Am J Ophthalmol*, (Mar 28, 1879-1891 (Electronic)
- Huang, D., Swanson, E.A., Lin, C.P., Schuman, J.S., Stinson, W.G., Chang, W., Hee, M.R., Flotte, T., Gregory, K., Puliafito, C.A. & et al. (1991). Optical coherence tomography. *Science*, Vol. 254, No. 5035, (Nov 22 1991) pp. (1178-1181), 0036-8075 (Print)
- Ishikawa, H., Liebmann, J.M. & Ritch, R. (2000). Quantitative assessment of the anterior segment using ultrasound biomicroscopy. *Curr Opin Ophthalmol*, Vol. 11, No. 2, (Apr 2000) pp. (133-139), 1040-8738 (Print)
- Izatt, J.A., Hee, M.R., Swanson, E.A., Lin, C.P., Huang, D., Schuman, J.S., Puliafito, C.A. & Fujimoto, J.G. (1994). Micrometer-scale resolution imaging of the anterior eye in vivo with optical coherence tomography. *Arch Ophthalmol*, Vol. 112, No. 12, (Dec 1994) pp. (1584-1589), 0003-9950 (Print)
- Jacobs, I.H. (1979). Anterior chamber depth measurement using the split-lamp microscope. *Am J Ophthalmol*, Vol. 88, No. 2, (Aug 1979) pp. (236-238), 0002-9394 (Print)
- Kanski, J.J. (2007). *Clinical ophthalmology: a systematic approach*, (6th), Butterworth Heinemann Elsevier, 9780080449692 (hbk.)
- Khor, W.B., Sakata, L.M., Friedman, D.S., Narayanaswamy, A., Lavanya, R., Perera, S.A. & Aung, T. Evaluation of scanning protocols for imaging the anterior chamber angle with anterior segment-optical coherence tomography. *J Glaucoma*, Vol. 19, No. 6, (Aug 365-368), 1536-481X (Electronic)

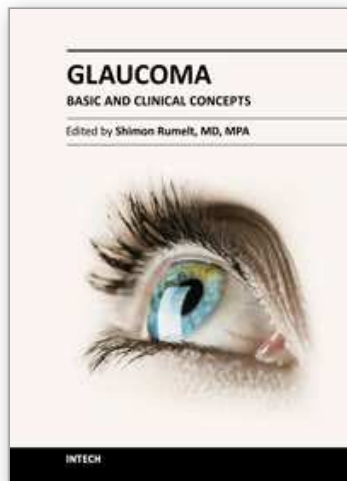
- Kim, Y.Y. & Jung, H.R. (1997). Clarifying the nomenclature for primary angle-closure glaucoma. *Surv Ophthalmol*, Vol. 42, No. 2, (Sep-Oct 1997) pp. (125-136), 0039-6257 (Print)
- Kurita, N., Mayama, C., Tomidokoro, A., Aihara, M. & Araie, M. (2009). Potential of the pentacam in screening for primary angle closure and primary angle closure suspect. *J Glaucoma*, Vol. 18, No. 7, (Sep 2009) pp. (506-512), 1536-481X (Electronic)
- Lam, A.K., Chan, R., Woo, G.C., Pang, P.C. & Chiu, R. (2002). Intra-observer and inter-observer repeatability of anterior eye segment analysis system (EAS-1000) in anterior chamber configuration. *Ophthalmic Physiol Opt*, Vol. 22, No. 6, (Nov 2002) pp. (552-559), 0275-5408 (Print)
- Larsen, J.S. (1971). The sagittal growth of the eye. 1. Ultrasonic measurement of the depth of the anterior chamber from birth to puberty. *Acta Ophthalmol (Copenh)*, Vol. 49, No. 2, 1971) pp. (239-262), 0001-639X (Print)
- Lens, A., Nemeth, S.C., Ledford, J.K. (2008). *Ocular Anatomy and Physiology*, (Second Edition), Slack Incorporated, 978-1-55642-792-3,
- Li, H., Leung, C.K., Cheung, C.Y., Wong, L., Pang, C.P., Weinreb, R.N. & Lam, D.S. (2007). Repeatability and reproducibility of anterior chamber angle measurement with anterior segment optical coherence tomography. *Br J Ophthalmol*, Vol. 91, No. 11, (Nov 2007) pp. (1490-1492), 0007-1161 (Print)
- Liang, J., Liu, W., Xing, X., Liu, H., Zhao, S. & Ji, J. Evaluation of the agreement between Pentacam and ultrasound biomicroscopy measurements of anterior chamber depth in Chinese patients with primary angle-closure glaucoma. *Jpn J Ophthalmol*, Vol. 54, No. 4, (Jul 361-362), 1613-2246 (Electronic)
- Mansouri, K., Sommerhalder, J. & Shaarawy, T. Prospective comparison of ultrasound biomicroscopy and anterior segment optical coherence tomography for evaluation of anterior chamber dimensions in European eyes with primary angle closure. *Eye (Lond)*, Vol. 24, No. 2, (Feb 233-239), 1476-5454 (Electronic)
- Marchini, G., Pagliarusco, A., Toscano, A., Tosi, R., Brunelli, C. & Bonomi, L. (1998). Ultrasound biomicroscopic and conventional ultrasonographic study of ocular dimensions in primary angle-closure glaucoma. *Ophthalmology*, Vol. 105, No. 11, (Nov 1998) pp. (2091-2098), 0161-6420 (Print)
- Mou, D., Fu, J., Li, S., Wang, L., Wang, X., Wu, G., Qing, G., Peng, Y. & Wang, N. Narrow- and open-angle measurements with anterior-segment optical coherence tomography and Pentacam. *Ophthalmic Surg Lasers Imaging*, Vol. 41, No. 6, (Nov 1 622-628), 1938-2375 (Electronic)
- Muller, M., Dahmen, G., Porksen, E., Geerling, G., Laqua, H., Ziegler, A. & Hoerauf, H. (2006). Anterior chamber angle measurement with optical coherence tomography: intraobserver and interobserver variability. *J Cataract Refract Surg*, Vol. 32, No. 11, (Nov 2006) pp. (1803-1808), 0886-3350 (Print)
- Ng, W.S., Ang, G.S. & Azuara-Blanco, A. (2008). Laser peripheral iridoplasty for angle-closure. *Cochrane Database Syst Rev*, No. 3, 2008) pp. (CD006746), 1469-493X (Electronic)
- Nolan, W.P., Baasanhu, J., Undraa, A., Uranchimeg, D., Ganzorig, S. & Johnson, G.J. (2003). Screening for primary angle closure in Mongolia: a randomised controlled trial to determine whether screening and prophylactic treatment will reduce the incidence of primary angle closure glaucoma in an east Asian population. *Br J Ophthalmol*, Vol. 87, No. 3, (Mar 2003) pp. (271-274), 0007-1161 (Print)

- Nolan, W.P., See, J.L., Chew, P.T., Friedman, D.S., Smith, S.D., Radhakrishnan, S., Zheng, C., Foster, P.J. & Aung, T. (2007). Detection of primary angle closure using anterior segment optical coherence tomography in Asian eyes. *Ophthalmology*, Vol. 114, No. 1, (Jan 2007) pp. (33-39), 1549-4713 (Electronic)
- Osuobeni, E.P., Hegarty, C. & Guvant, P. (2003). The effect of central corneal thickness on estimates of the anterior chamber depth. *Clin Exp Optom*, Vol. 86, No. 6, (Nov 2003) pp. (371-375), 0816-4622 (Print)
- Osuobeni, E.P., Oduwaiye, K.A. & Ogbuehi, K.C. (2000). Intra-observer repeatability and inter-observer agreement of the Smith method of measuring the anterior chamber depth. *Ophthalmic Physiol Opt*, Vol. 20, No. 2, (Mar 2000) pp. (153-159), 0275-5408 (Print)
- Pavlin, C.J., Harasiewicz, K. & Foster, F.S. (1992). Ultrasound biomicroscopy of anterior segment structures in normal and glaucomatous eyes. *Am J Ophthalmol*, Vol. 113, No. 4, (Apr 15 1992) pp. (381-389), 0002-9394 (Print)
- Pekmezci, M., Porco, T.C. & Lin, S.C. (2009). Anterior segment optical coherence tomography as a screening tool for the assessment of the anterior segment angle. *Ophthalmic Surg Lasers Imaging*, Vol. 40, No. 4, (Jul-Aug 2009) pp. (389-398), 1542-8877 (Print)
- Quek, D.T., Nongpiur, M.E., Perera, S.A. & Aung, T. Angle imaging: advances and challenges. *Indian J Ophthalmol*, Vol. 59 Suppl, (Jan S69-75), 1998-3689 (Electronic)
- Quigley, H.A. & Broman, A.T. (2006). The number of people with glaucoma worldwide in 2010 and 2020. *Br J Ophthalmol*, Vol. 90, No. 3, (Mar 2006) pp. (262-267), 0007-1161 (Print)
- Rabsilber, T.M., Khoramnia, R. & Auffarth, G.U. (2006). Anterior chamber measurements using Pentacam rotating Scheimpflug camera. *J Cataract Refract Surg*, Vol. 32, No. 3, (Mar 2006) pp. (456-459), 0886-3350 (Print)
- Radhakrishnan, S., Goldsmith, J., Huang, D., Westphal, V., Dueker, D.K., Rollins, A.M., Izatt, J.A. & Smith, S.D. (2005). Comparison of optical coherence tomography and ultrasound biomicroscopy for detection of narrow anterior chamber angles. *Arch Ophthalmol*, Vol. 123, No. 8, (Aug 2005) pp. (1053-1059), 0003-9950 (Print)
- Ritch, R., Tham, C.C. & Lam, D.S. (2007). Argon laser peripheral iridoplasty (ALPI): an update. *Surv Ophthalmol*, Vol. 52, No. 3, (May-Jun 2007) pp. (279-288), 0039-6257 (Print)
- Rufer, F., Schroder, A., Klettner, A., Frimpong-Boateng, A., Roider, J.B. & Erb, C. Anterior chamber depth and iridocorneal angle in healthy White subjects: effects of age, gender and refraction. *Acta Ophthalmol*, Vol. 88, No. 8, (Dec 885-890), 1755-3768 (Electronic)
- Sakata, L.M., Lavanya, R., Friedman, D.S., Aung, H.T., Gao, H., Kumar, R.S., Foster, P.J. & Aung, T. (2008a). Comparison of gonioscopy and anterior segment ocular coherence tomography in detecting angle closure in different quadrants of the anterior chamber angle. *Ophthalmology*, Vol. 115, No. 5, (May 2008a) pp. (769-774), 1549-4713 (Electronic)
- Sakata, L.M., Lavanya, R., Friedman, D.S., Aung, H.T., Seah, S.K., Foster, P.J. & Aung, T. (2008b). Assessment of the scleral spur in anterior segment optical coherence tomography images. *Arch Ophthalmol*, Vol. 126, No. 2, (Feb 2008b) pp. (181-185), 0003-9950 (Print)

- Scheie, H.G. (1957). Width and pigmentation of the angle of the anterior chamber; a system of grading by gonioscopy. *AMA Arch Ophthalmol*, Vol. 58, No. 4, (Oct 1957) pp. (510-512), 0096-6339 (Print)
- See, J.L., Chew, P.T., Smith, S.D., Nolan, W.P., Chan, Y.H., Huang, D., Zheng, C., Foster, P.J., Aung, T. & Friedman, D.S. (2007). Changes in anterior segment morphology in response to illumination and after laser iridotomy in Asian eyes: an anterior segment OCT study. *Br J Ophthalmol*, Vol. 91, No. 11, (Nov 2007) pp. (1485-1489), 0007-1161 (Print)
- Shaffer, R.N. (1960). Primary glaucomas. Gonioscopy, ophthalmoscopy and perimetry. *Trans Am Acad Ophthalmol Otolaryngol*, Vol. 64, (Mar-Apr 1960) pp. (112-127), 0002-7154 (Print)
- Sihota, R., Dada, T., Gupta, R., Lakshminarayan, P. & Pandey, R.M. (2005). Ultrasound biomicroscopy in the subtypes of primary angle closure glaucoma. *J Glaucoma*, Vol. 14, No. 5, (Oct 2005) pp. (387-391), 1057-0829 (Print)
- Smith, R.J. (1979). A new method of estimating the depth of the anterior chamber. *Br J Ophthalmol*, Vol. 63, No. 4, (Apr 1979) pp. (215-220), 0007-1161 (Print)
- Spaeth, G.L. (1971). The normal development of the human anterior chamber angle: a new system of descriptive grading. *Trans Ophthalmol Soc U K*, Vol. 91, 1971) pp. (709-739), 0078-5334 (Print)
- Spaeth, G.L., Aruajo, S. & Azuara, A. (1995). Comparison of the configuration of the human anterior chamber angle, as determined by the Spaeth gonioscopic grading system and ultrasound biomicroscopy. *Trans Am Ophthalmol Soc*, Vol. 93, 1995) pp. (337-347; discussion 347-351), 0065-9533 (Print)
- Tan, A.N., Sauren, L.D., de Brabander, J., Berendschot, T.T., Passos, V.L., Webers, C.A., Nuijts, R.M. & Beckers, H.J. Reproducibility of anterior chamber angle measurements with anterior segment optical coherence tomography. *Invest Ophthalmol Vis Sci*, Vol. 52, No. 5, 2095-2099), 1552-5783 (Electronic)
- Thomas, R., George, R., Parikh, R., Muliyl, J. & Jacob, A. (2003a). Five year risk of progression of primary angle closure suspects to primary angle closure: a population based study. *Br J Ophthalmol*, Vol. 87, No. 4, (Apr 2003a) pp. (450-454), 0007-1161 (Print)
- Thomas, R., George, T., Braganza, A. & Muliyl, J. (1996). The flashlight test and van Herick's test are poor predictors for occludable angles. *Aust N Z J Ophthalmol*, Vol. 24, No. 3, (Aug 1996) pp. (251-256), 0814-9763 (Print)
- Thomas, R., Parikh, R., Muliyl, J. & Kumar, R.S. (2003b). Five-year risk of progression of primary angle closure to primary angle closure glaucoma: a population-based study. *Acta Ophthalmol Scand*, Vol. 81, No. 5, (Oct 2003b) pp. (480-485), 1395-3907 (Print)
- Ursea, R. & Silverman, R.H. Anterior-segment imaging for assessment of glaucoma. *Expert Rev Ophthalmol*, Vol. 5, No. 1, (Feb 1 59-74), 1746-9899 (Electronic)
- Van Herick, W., Shaffer, R.N. & Schwartz, A. (1969). Estimation of width of angle of anterior chamber. Incidence and significance of the narrow angle. *Am J Ophthalmol*, Vol. 68, No. 4, (Oct 1969) pp. (626-629), 0002-9394 (Print)
- Wang, D., Pekmezci, M., Basham, R.P., He, M., Seider, M.I. & Lin, S.C. (2009). Comparison of different modes in optical coherence tomography and ultrasound biomicroscopy in anterior chamber angle assessment. *J Glaucoma*, Vol. 18, No. 6, (Aug 2009) pp. (472-478), 1536-481X (Electronic)

- Wishart, P.K. & Batterbury, M. (1992). Ocular hypertension: correlation of anterior chamber angle width and risk of progression to glaucoma. *Eye (Lond)*, Vol. 6 (Pt 3), 1992) pp. (248-256), 0950-222X (Print)
- Wong, H.T., Lim, M.C., Sakata, L.M., Aung, H.T., Amerasinghe, N., Friedman, D.S. & Aung, T. (2009). High-definition optical coherence tomography imaging of the iridocorneal angle of the eye. *Arch Ophthalmol*, Vol. 127, No. 3, (Mar 2009) pp. (256-260), 1538-3601 (Electronic)
- Yoo, C., Oh, J.H., Kim, Y.Y. & Jung, H.R. (2007). Peripheral anterior synechiae and ultrasound biomicroscopic parameters in angle-closure glaucoma suspects. *Korean J Ophthalmol*, Vol. 21, No. 2, (Jun 2007) pp. (106-110), 1011-8942 (Print)

IntechOpen



Glaucoma - Basic and Clinical Concepts

Edited by Dr Shimon Rumelt

ISBN 978-953-307-591-4

Hard cover, 590 pages

Publisher InTech

Published online 11, November, 2011

Published in print edition November, 2011

This book addresses the basic and clinical science of glaucomas, a group of diseases that affect the optic nerve and visual fields and is usually accompanied by increased intraocular pressure. The book incorporates the latest development as well as future perspectives in glaucoma, since it has expedited publication. It is aimed for specialists in glaucoma, researchers, general ophthalmologists and trainees to increase knowledge and encourage further progress in understanding and managing these complicated diseases.

How to reference

In order to correctly reference this scholarly work, feel free to copy and paste the following:

Claudio Campa, Luisa Pierro, Paolo Bettin and Francesco Bandello (2011). Anterior Chamber Angle Assessment Techniques, *Glaucoma - Basic and Clinical Concepts*, Dr Shimon Rumelt (Ed.), ISBN: 978-953-307-591-4, InTech, Available from: <http://www.intechopen.com/books/glaucoma-basic-and-clinical-concepts/anterior-chamber-angle-assessment-techniques>

INTECH
open science | open minds

InTech Europe

University Campus STeP Ri
Slavka Krautzeka 83/A
51000 Rijeka, Croatia
Phone: +385 (51) 770 447
Fax: +385 (51) 686 166
www.intechopen.com

InTech China

Unit 405, Office Block, Hotel Equatorial Shanghai
No.65, Yan An Road (West), Shanghai, 200040, China
中国上海市延安西路65号上海国际贵都大饭店办公楼405单元
Phone: +86-21-62489820
Fax: +86-21-62489821

© 2011 The Author(s). Licensee IntechOpen. This is an open access article distributed under the terms of the [Creative Commons Attribution 3.0 License](#), which permits unrestricted use, distribution, and reproduction in any medium, provided the original work is properly cited.

IntechOpen

IntechOpen